

A Superconducting Magnet System for Whole-Body Metabolism Imaging

Q. Wang, Y. Dai, B. Zhao, S. Song, C. Wang, L. Li, J. Cheng, S. Chen, H. Wang, Z. Ni, Y. Li, C. Cui, X. Hu, H. Wang, Y. Lei, K. Chan, L. Yan, C. Wen, G. Hui, W. Yang, F. Liu, Y. Zhuo, X. Zhou, Z. Yan, J. Chen, and T. Xu

Abstract—A 9.4 Tesla superconducting magnet is designed and fabricated with a warm bore of 800 mm for neuroscience research. The superconducting magnet will be made of a NbTi Wire-in-Channel (WIC) conductor with a higher ratio of copper to non-copper, which thus sustains the high stresses. It is cooled to operate temperature at 4.2 K liquid helium. The cryostat system is cooled through GM cryocoolers, some used to cool the radiation shield, and the others realize the re-condensed liquid helium. The MRI magnet system has a high level of stored energy, about 134 MJ, and a relatively-lower nominal current, about 212.5 A. The magnet will be operated in a persistent current mode with a superconducting switch. The WIC wires are employed to meet the cryostability criteria to avoid any risks from quench. The protection circuit with the subdivision of the coil reduces the terminate voltage and hot-spot temperature. In the paper, the specifications of magnet system will be presented.

Index Terms—Metabolism imaging, MRI superconducting magnet, passive shield, sub-division quench protection.

I. INTRODUCTION

THE MRI provides a clear anatomical structure to reveal the physiological state of tissues and functional activity. Over the past 30 years [1], it has been developed into one of the most important tools for medical imaging, and brain and cognitive science. So far, all MRI systems are designed with proton magnetic resonance signals as the starting point, but the information carried by the hydrogen in the water molecules is of little use for the metabolism. In fact, ^{23}Na , ^{31}P and other metabolics with a wealth of information can also provide non-proton nuclide magnetic resonance signals, but it is necessary to overcome the problem of a low signal-to-noise ratio (SNR). With the increment of the magnetic field strength, the magnetic resonance

Manuscript received September 09, 2011; accepted November 07, 2011. Date of publication November 14, 2011; date of current version May 24, 2012. This work was supported in part by the Important Scientific instrument Project of CAS; Nature Science Found Chinese 50925726.

Q. Wang, Y. Dai, B. Zhao, S. Song, C. Wang, L. Li, J. Cheng, S. Chen, H. Wang, Z. Ni, Y. Li, C. Cui, X. Hu, C. Yi, H. Wang, Y. Lei, K. Chan, L. Yan, Z. Dong, C. Wen, G. Hui, and W. Yang are with the Institute of Electrical Engineering, CAS, Beijing 100190, China (e-mail: qiuliang@mail.iee.ac.cn).

F. Liu is with the University of Queensland, Brisbane, QLD 4072, Australia (e-mail: Feng@itee.uq.edu.au).

Y. Zhuo is with the Institute of Biophysics, Chinese Academy of Sciences, Beijing 100190, China.

X. Zhou, Z. Yan, J. Chen, and T. Xu are with the Institute of Biophysics CAS, Beijing 100190, China (e-mail: jingchen@bcslab.ibp.ac.cn).

Color versions of one or more of the figures in this paper are available online at <http://ieeexplore.ieee.org>.

Digital Object Identifier 10.1109/TASC.2011.2175888

TABLE I
SPECIFICATIONS FOR THE MAGNET SYSTEM

Magnet type	NbTi superconducting magnet
Magnetic field	9.4 Tesla
Shield type	Passive shield
Stability of magnetic field	≤ 0.03 ppm/h
Shimming magnetic field	Superconducting coil shims, room shims and passive iron piece shims
Homogeneity (RMS)	
22 cm DSV	≤ 0.05 ppm
30 cm DSV	≤ 0.1 ppm
5 G line (B_z and B_r)	$\leq 22 \text{ m} \times 18 \text{ m}$ (no passive shield)
Magnet length	$\sim 3.5 \text{ m}$
Warm bore diameter	$\geq 800 \text{ mm}$
Weight of magnet (including 100% LHe)	$\leq 50 \text{ ton}$
Cooling method	Zero boiling off liquid helium

SNR is enhanced. It is possible to clearly obtain non-proton nuclide imaging, such as, ^{23}Na , ^{31}P , to reveal the metabolic processes of biological systems [2].

Compared with the commercially available 0.5 ~ 3 T MRI [3], a high magnetic field MRI with a central field of 9.4 T has some advantages. It can achieve a higher resolution for observing the fine structure and function of the boundaries of the nuclei and a higher spectral resolution more than three times that of a 3 T system.

This paper describes a 9.4 T superconducting magnet which is being developed in Institute of Electrical Engineering, Chinese Academy of Science. The magnet is with a warm bore size of 800 mm in diameter, and zero boiling-off liquid helium will be used for cooling the superconductors. The magnet system is designed and fabricated from 2011 to 2014.

II. ELECTROMAGNETIC STRUCTURE FOR MRI MAGNET

The specifications for the magnet system are listed in Table I. The design of a MRI magnet involves a complex iterative process in which a balance must often be made between the conflicting requirements of the bore size, homogeneity, management of mechanical stress, stability and cost.

The superconducting main coils generate the central magnetic field. The compensating coils shim the magnetic field uniformity in the diameter spherical volume (DSV) to meet the requirements of the MRI. The configuration with the coaxial solenoid-shaped coil and symmetrical compensating coils through the cascade of different winding current densities is selected to minimize the maximum magnetic field and the hoop stress. The

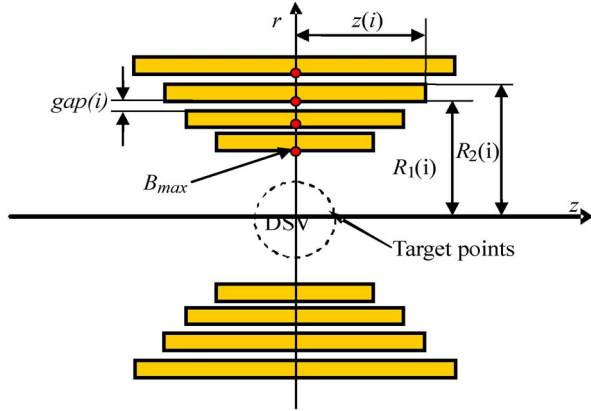


Fig. 1. Optimal calculation model of coil.

whole magnet system is designed with the minimum cost of consumption and magnetic energy storage as the objective functions. According to the characteristics of the NbTi superconductor, it is necessary to reduce construction cost by the same material with different specifications. The graded current density in the coils is based on the critical current curves ($B - J$ characteristic curve) with the local fields [4]. If all coils have the same power supply, the safety factors should be the same for each winding.

MRI magnets operate in the persistent-current-mode and the coils are in series with the same operating current. Based on almost the same safety factor and the relation of the magnetic field-current, the different sizes superconducting wires are selected to achieve different operating current densities in each coil. To reduce the system cost, the volume of the superconductors should be minimized. As shown in Fig. 1, the optimal design is based on the following model:

$$\begin{aligned} \text{Objective function} \quad & \text{Min} \sum_{i=1}^N v_i \\ \text{Subjected to} \quad & \begin{cases} R_1(i) < R_2(i) \\ R_2(i) + \text{gap}(i) \leq R_1(i+1) \\ |(B_i - B_0)/B_0| < \varepsilon \\ j_{\text{opt}}/j_c < \eta \\ l_b \leq x \leq u_b \end{cases} \end{aligned} \quad (1)$$

where η is the current margin, v_i is the volume of each coil, B_0 is the center field, B_i is the field of each point located in the region of DSV, j_{opt} and j_c are the operating and critical current densities, N is the number of subdivisions for the main coil, u_b and l_b are for the variables x in the upper and lower limits, $x = [R_1(i), R_2(i), Z(i); i = 1, 2, \dots, N]$ are the optimization variables, where R_1, R_2, Z are the inner, outer radius and half height of each coil. The gaps between the coils (gap) are used for a bobbin and assembly and reinforcement.

To obtain high homogeneity field, the uniformity constraint in the DSV is needed. Usually, the initial value is assumed to be about $\varepsilon = 10^{-3}$. This is a nonlinear optimization problem that includes both the linear and nonlinear constraints. The problem will be solved through using successive quadratic programming (SQP) algorithm. The specifications of the main coils are optimized [4]. Because the homogeneity of magnetic field in the

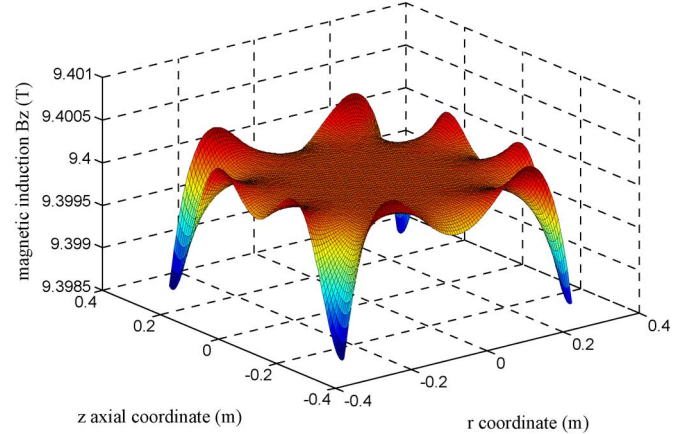


Fig. 2. Field distribution in the DSV.

TABLE II
SPECIFICATIONS OF SUPERCONDUCTING MAGNET

Operating current	212.5 A
Central field	9.4 T
Maximum magnetic field	9.5 T
Number of coils	13
Homogeneity in 30 cm	0.1 ppm
Coil length	3.0 m
Clear bore size/warm bore size	Φ910 mm/800 mm
Inductance	5939.3 H
Stored energy	134 MJ
Diameter of coil	1579 mm
5 G line	r=17 m, z=22 m

main coils cannot meet the requirements of MRI, the non-uniform component will be annulled with compensating coils. A continuous current linear-nonlinear optimal method is proposed for the design of the parameters [5].

The initial structure of the optimization with the subdivision of the solenoid into five coils leads to an easy fabrication. The consumption of wire reduces with the increment of the operating current. The hoop stress of the coil increases with increment of the operating current. This is because with the same size of wire, the increment of the operating current leads to a large current density and magnetic field. Therefore, the hoop stress with respect to the operating current density is proportional to the square of j_{opt} . In the design, the main magnet is subdivided into nine coaxial coils. The nine coils are divided into five groups and each coil can be wound on a bobbin. Four compensating coils can be located at the outermost layer of the main coil. The structures are based on the available conductor length to easily fabricate the actual winding. The parameters of the magnet are listed in Table II, the homogeneity of magnetic field is better than 0.1 ppm in the DSV in 300 mm, the maximum magnetic field is only 9.5 T located at the inner winding. The magnetic field distribution of the central region is shown in Fig. 2, the stray field of the magnet is the 5 Gauss line about 17 m and the axial direction less than 22 m.

III. CONDUCTOR FOR THE SUPERCONDUCTING COIL

The wires are selected on the basis of the safety, mechanical structure, manufacturing process and power supply.

TABLE III
SPECIFICATIONS OF WIRE AND OPERATING CONDITIONS

	Wire area (mm ²)	Cu/SC (-)	B_{max} (T)	$T_{cs}-T_b$ (K)	J_{opt} (A/mm ²)
1	2.38×4.48	6	9.498	0.50	19.161
2	2.38×4.48	6	8.940	0.60	19.161
3	2.25×3.49	10	8.432	1.03	25.931
4	2.25×3.49	10	7.598	1.23	25.931
5	2.25×3.49	17	6.845	1.68	25.931
6	2×3.25	18	5.653	2.17	31.228
7	2×3.25	18	5.510	2.18	31.228
8	1.59×2.94	12	5.313	1.92	43.035
9	1.43×2.24	7	5.280	1.58	62.425
10	1.37×1.95	10	4.879	1.20	74.512
11	1.37×1.95	10	1.411	2.77	-74.905

A. Superconducting Wire-in-Channel

The superconducting wire is critical to the high magnetic field coils. The performance of the superconducting magnets is related to the critical characteristics of superconducting wire. According to the design, the operating current densities for the coils are listed in Table III. All 9 main coils have the same length of 3 m and the main and compensating coils are in series with a power supply. To meet the requirements of the current density, the size and critical current of wire were chosen to meet the different current densities in each winding.

B. Margin of Operation

The stability and operating current of superconducting wire are varied with the ratio of the copper to the superconductor (Cu/SC). The conductor with the higher Cu/SC ratio is the more stable, but, the critical current is lower. It should be determined according to the operating margins of the magnet. The characteristics of superconducting wire are listed in Table III.

There are eight kinds of wire. All the wires are wire-in-channel (WIC). The type of wire can achieve a high stability. The compensating coils are located at the low field region.

The temperature margin ($\Delta T = T_{cs} - T_b$) of the coil depends on the nominal current, magnetic field and critical properties. All coils work the same current of 212.5 A. The temperature margins listed in Table III are different because of the location and magnetic field of the different wires in the coil using the different critical characteristics. The coils 1 and 2 have the minimum temperature margins about 0.5 K and 0.6 K, because of the inner coil with the magnetic field strength of 9.5 T. The higher temperature margins are located at the outer coils.

IV. STRESS ANALYSIS FOR SUPERCONDUCTING MAGNETS

The Lorentz force acts directly on the superconducting wire during the normal operation of magnet. The inhomogeneous stress distribution exists in the conductor, filling material and insulation material. The mechanical properties of the superconductors are an important factor affecting the critical properties. In particular, the superconducting magnets with the high magnetic field of 9.4 T, large clear diameter of 910 mm, and superconducting wires may suffer plastic deformation. Thus, the serious degradation of the critical features will affect the stability of the magnet. It is necessary to understand the mechanical

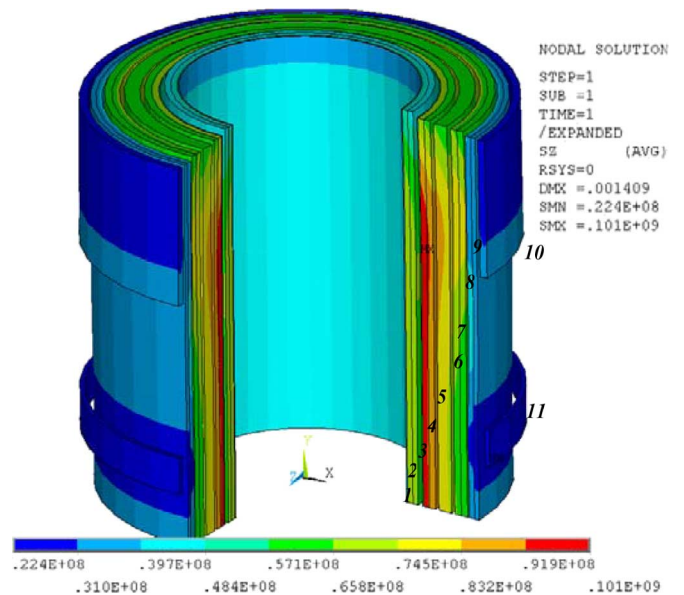


Fig. 3. Hoop stress in superconducting coils for the 9.4 T MRI (unit: Pa).

stresses, electromagnetic forces and dynamic stresses during quench.

The calculation of the equivalent elastic parameters, such as Young's modulus, Poisson ratio and shear modulus in the superconducting coils, is based on the micro-mechanics theory for composites. The averaged material characteristics of the magnet are calculated according to the parameters of a single material. As shown in Fig. 3, the maximum hoop stress of the magnet is about 101 MPa in the wire in coil-3.

The maximum hoop strain of the winding is 0.16%, which is an important parameter for the stability of the magnet. Because if the strain is too large, the critical current of the superconducting wire is degraded, usually it has been assumed that it is safe if the hoop strain is below 0.2%. Therefore, the calculations indicated that the design is safe in this aspect. According the averaged model, the maximum hoop stress is calculated. To obtain accuracy stress distribution in the highest stress coil-3, it is necessary to use the detailed model of the finite element method for further analysis of the detailed stress distribution in the wire. The development of an equivalent force model with the hierarchical group structure refinement mesh finite element elastic-plastic technology is a more efficient and accurate calculation of the stress distribution in the high field magnet. Epoxy glass cloth reinforced with a thickness of 0.03 mm is located between each wire. The glass fiber-reinforced epoxy material parameters are according to the parameters given, and banding stainless steel wire. Fig. 4 shows the hoop stress distribution in the conductor. The maximum hoop stress in the Wire-In-Channel conductor is about 131.1 MPa.

V. QUENCH PROTECTION FOR SUPERCONDUCTING MAGNET

The protection circuit is designed with combined active and passive methods. The active quench protection system includes a quench detection subsystem and data acquisition. It can provide the data for the quench analysis and quickly triggers the heaters. The passive protection methods will divide the

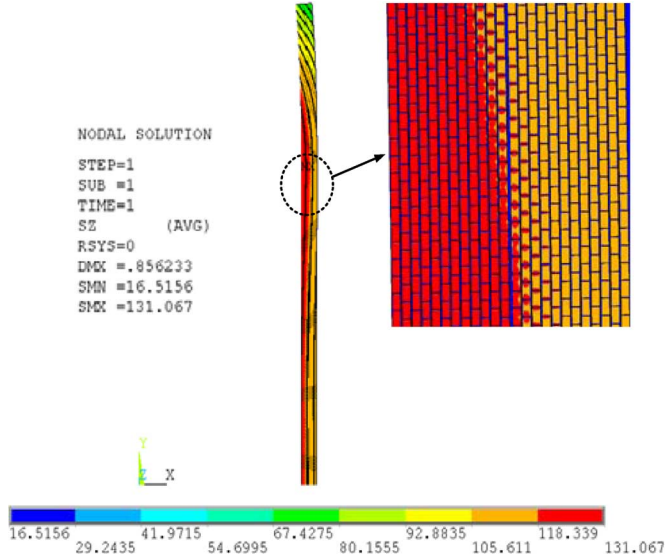


Fig. 4. Hoop stress with the hierarchical group structure refinement mesh finite element elastic-plastic technology in coil-3 (unit: MPa).

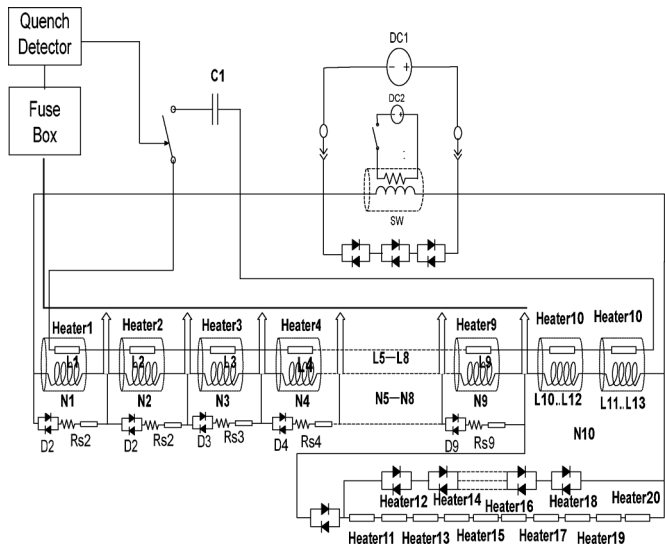


Fig. 5. Protection circuit. Numbers of coils are shown in Fig. 4 and C1 is electrical capacity for trigger the heaters.

coils into multi-sections. These are in series and parallel with the back-to-back diodes and resistors. The active protection is through comparing the voltages methods to detect the quench. The terminating voltage is also analyzed quickly and accurately to determine whether the magnet quench occurred. The passive protection method is the subdivision of the coils into 10 segments due to high terminate. The coils 10, 11, 12 and 13 are the same circuit, as shown in Fig. 5. After the quench of the coil for the first time, the heater will trigger the other coils to quench. Heaters with a width of 5 cm and thickness of 1 mm and the same length as the coils will be installed outside of the coil. The quench simulation results for hot-spot temperatures are plotted respectively in Fig. 6.

It shows the acceptable values for the maximum temperature of 120 K, the maximum voltage of 300 V and the maximum induced current of 350 A. By adjusting the subdivision number,

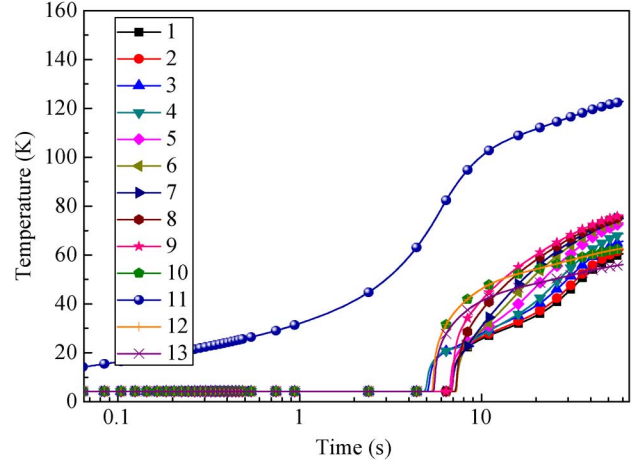


Fig. 6. Profiles of hot-spot temperature in coils after the first quench of No. 11.

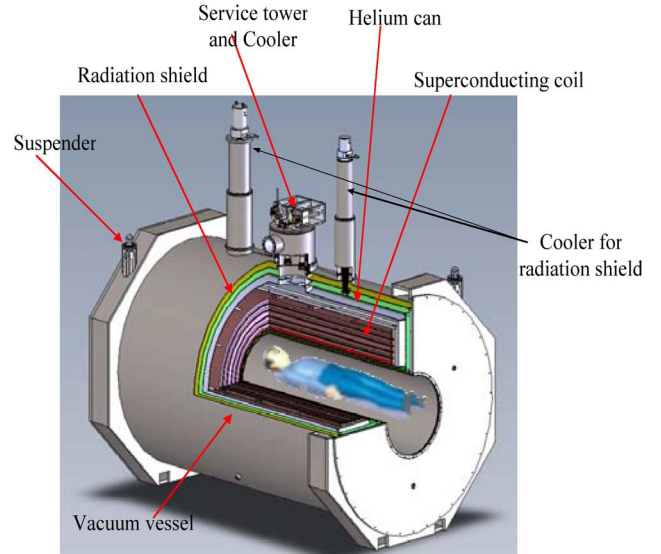


Fig. 7. Configuration of cryostat for 9.4 T MRI.

protection resistors, heater and heating power and position of the heaters, the hot-spot temperature, induced current and terminate voltage can be reduced. The induced current during the quench of the coil generates the variable stresses in each coil. It is necessary to evaluate the dynamic stress to check the allowance stress region. According to the quench simulation, the profiles of the stress with respect to time are calculated. The maximum stress during quench is about 130 MPa.

VI. CRYOSTAT

The liquid helium cryostat is made from austenitic stainless steel. To reduce heat leakage, there are two layers of aluminum shielding. The radiation shields were linked with the cryocooler through the soft copper wires. Multi-layer insulation (MLI) can further reduce the thermal radiation. The re-condenser cooler is installed in the cold tower in the upper part of the vacuum vessel. The vacuum vessel with the high vacuum to eliminate heat transfer and reduce the thermal conductivity of gas is located outside radiation shield and liquid helium can. An octagonal-shape beam supports the cold weight. The race-track shape

rod made of E-glass epoxy FRP has a very low thermal conductivity. The weight hangs through the rigid race-track shape rod of the four groups. The upper part of the vacuum vessel is equipped with a service cooling tower of a double layer structure. The lower part of the neck is welded to the liquid helium vessel and the outside neck is connected to the vacuum vessel. The current leads, helium transfer pipes, measuring leads and two cryocoolers are all located in the service tower. The condenser connected to the cryocooler is cooling helium gas to realize zero boiling off liquid helium. Fig. 7 is the configuration of the cryostat.

The liquid helium vessel with a volume of 6479 L can contain liquid with a volume of 2908 L. After the quench, the internal pressure depends on the burst valve. The radiation shields fabricated by aluminum alloy with a high thermal conductivity and high strength are installed outside the container of liquid helium. A shield of 50 K is connected to the single-stage GM cryocoolers through the soft copper.

VII. CONCLUSION

A superconducting magnet is designed for an MRI with a center field of 9.4 T and a warm-bore size of 800 mm. The

optimal specifications of the magnet can generate the magnetic field with the homogeneity of 0.1 ppm in 300 mm DSV. The analyses of the quench and stress show that the magnet is very stable and safe. The cryostat with cryocoolers for the radiation shield and recondensed helium can realize the operation.

REFERENCES

- [1] Y. Lvovski and P. Jarvis, "Superconducting system for MRI-present solutions and new trends," *IEEE Trans. Appl. Supercond.*, vol. 15, pp. 1317–1325, 2005.
- [2] P.-M. Robitaille and L. Berliner, *Ultra High Field Magnetic Resonance Imaging*. : Springer, 2006.
- [3] M. Lakrimi and A. M. Thomas *et al.*, "The principles and evolution of magnetic resonance imaging," *J. of Physics: Conf.*, vol. 286, pp. 1–11, 2011.
- [4] C. Wang, Q. Wang, and Q. Zhang, "Multiple layer superconducting magnet design for magnetic resonance imaging," *IEEE Trans. Appl. Supercond.*, vol. 20, no. 3, pp. 706–709, 2010.
- [5] Q. Wang and G. Xu *et al.*, "Design of open high magnetic field MRI superconducting magnet with continuous current and genetic algorithm method," *IEEE Trans. Appl. Supercond.*, vol. 19, pp. 2289–2292, 2009.